

Chaos in Overhead Travelling Cranes Load Motion

Jerzy MARGIELEWICZ*, Damian GAŚKA**, Tadeusz OPASIAK***, Tomasz HANISZEWSKI****

*Silesian University of Technology, Krasińskiego 8,40-019 Katowice, Poland, E-mail:jerzy.margielewicz@polsl.pl

**Silesian University of Technology, Krasińskiego 8,40-019 Katowice, Poland, E-mail:damian.gaska@polsl.pl

***Silesian University of Technology, Krasińskiego 8,40-019 Katowice, Poland, E-mail:tadeusz.opasiak@polsl.pl

****Silesian University of Technology, Krasińskiego 8,40-019 Katowice, Poland, E-mail:tomasz.haniszewski@polsl.pl

crossref <http://dx.doi.org/10.5755/j01.mech.25.3.21317>

1. Introduction

Heavy-duty machines, in particular cranes, carry out the tasks of transporting goods from one place to another. When moving loads, operators are often forced to bypass obstacles on the way. Operational mechanisms and high operating speeds cause unbalance of the load from the equilibrium position. Information about the dynamics of the load while transportation, play an important role in the context of its positioning and control of mechanisms [1, 2]. At the same time, the limitation of the swing has a decisive effect on the manoeuvrability, thus minimizing the effect of cargo collision with fixed obstacles [3-5]. From a theoretical point of view, the dynamics of the load is most easily reproduced through the mathematical pendulum model [6-8]. This approach is only a certain approximation of the actual conditions, and taking into account the vibrations of the load-carrying crane structure or rope susceptibility, causes that the model receives a strongly non-linear character. The published results of model tests have shown the possibility of chaotic vibrations in such a system if the system is activated by excitation with sufficiently high amplitude values of external load [8].

To evaluate the dynamic properties of nonlinear systems, a variety of tools may be used. The most effective and the most frequently used are numerical methods that allow estimation of the largest Lyapunov exponent [9], bifurcation diagrams [10], Fast Fourier Transform [11] and Poincare cross-sections [12]. In general terms Lyapunov exponents are defined by means of numerical coefficients, which characterize the increase of the distance measured between trajectories initially located in close proximity, observed on the phase plane. Through them, it is possible to determine the average rate of convergence or divergence of numerical solutions of differential equations. They are therefore a measure of the sensitivity of the solution to the initial conditions set. If the phase trajectories converge over time, then all exponents take values less than zero. The value of the exponents has a significant effect on the rate of transient damping, the smaller they are the faster the phenomenon goes [13]. If in the fixed motion of one Lyapunov exponent assumes a zero value, then the system is steady. Chaotic motion takes place when at least one of the exponents is positive. Bifurcation diagrams provide quantitative and qualitative information on period doubling. In this place, it is worth mentioning that the term bifurcations in chaos theory is understood as a division of the path of solutions [9]. Fourier transform is one of the most popular tools for analysing linear and nonlinear dynamic systems. Its basic purpose is

spectral analysis, which consists in estimating the parameters and properties of the time sequence by spreading it to the harmonics of the amplitude-frequency spectrum. At the same time, this transformation is based on a mathematical apparatus, trigonometric or complex Fourier series, and its complete transformation. When transforming the time-to-frequency signal, the Parseval theorem says that the energy contained in the temporal representation is equal to the energy in the frequency domain. The amplitude-frequency spectra of the chaotic behaviour of the system take on a continuous form, i.e., the whole series of harmonics is excited. Poincare maps are created when the trajectory passes through a fixed plane at regular intervals. The reference plane is determined in such a way as to provide as much information as possible about the solutions of the analysed equations of motion. In the case of periodic oscillations on the Poincare cross-section points are obtained, that can be located in different areas of the phase plane. Based on the number of points in the Poincare section, it is possible to identify the nature of the solution. In case of one-period oscillations in the plane one point is visible, while two points indicate the two-period oscillations. Chaotic vibrations on Poincare map appear as a set of points whose graphical image is composed of shapes called attractors.

2. Formulation of a mathematical model

When formulating a computational model, the following simplification assumptions were adopted. The influence of mechanical vibration of the overhead travelling crane structure was mapped by the harmonic kinematic force acting on the joint point of the rope to the drum „O”. Whereas the element moving in the guides, depicting the movement of the crane bridge, was treated as a massless. In addition, large oscillations in the plane of load fluctuations and energy losses at the rope attachment point were assumed. However, the susceptibility of the rope on which the transported load is suspended was omitted. A schematic representation of the examined phenomenological model is presented in the Fig. 1.

Based on the formulated dynamic load motion model (Fig. 1), the differential equations of motion are derived and take the form:

$$ml^2 \frac{d^2\varphi}{dt^2} + b \frac{d\varphi}{dt} + ml\omega_w^2 A \cos(\omega_w t) \sin(\varphi) + mg \sin(\varphi) = 0. \quad (1)$$

After entering the dimensionless time, the equation

of motion of the analysed system takes the form:

$$\frac{d^2\varphi}{d\tau^2} + \beta \frac{d\varphi}{d\tau} + [1 + \omega^2 p \cos(\omega\tau)] \sin(\varphi) = 0, \quad (2)$$

where: $\omega_0 = \sqrt{\frac{g}{l}}$, $\tau = \omega_0 t$, $\beta = \frac{b}{ml\sqrt{gl}}$, $p = \frac{A}{l}$, $\omega = \frac{\omega_w}{\omega_0}$

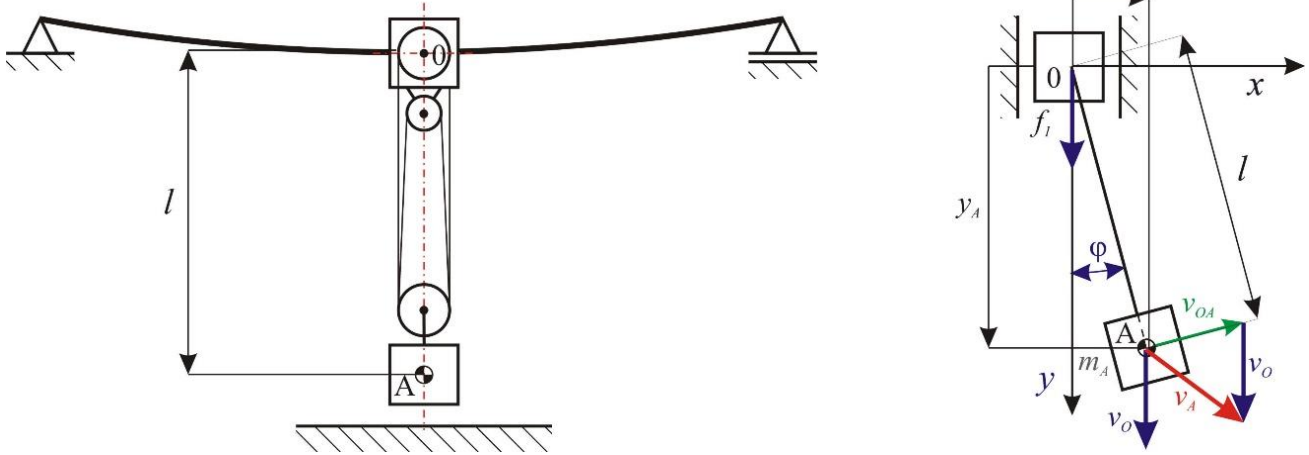


Fig. 1 The phenomenological model of the overhead travelling crane

To illustrate the course of a field line on a phase plane, the nonlinear second order equation of motion is transformed into a system of two first order equations:

$$\begin{cases} \frac{d\varphi}{d\tau} = v \\ \frac{dv}{d\tau} = -\beta \frac{d\varphi}{d\tau} - [1 + \omega^2 p \cos(\omega\tau)] \sin(\varphi) \end{cases} \quad (3)$$

On the other hand, the position of the load at any moment of time is determined by the equations of the constraints:

$$x_A = l \sin(\varphi), y_A = f_1 + l \cos(\varphi) = p \cos(\omega t) + l \cos(\varphi).$$

In the case when the impact of crane vibrations is omitted, the mathematical model (1) is reduced to the form:

$$\frac{d^2\varphi}{d\tau^2} + \beta \frac{d\varphi}{d\tau} + \sin(\varphi) = p \cos(\omega\tau), \quad (4)$$

where: $\omega_0 = \sqrt{\frac{g}{l}}$, $\tau = \omega_0 t$, $\beta = \frac{b}{ml^2 \omega_0}$,

$$p = \frac{M}{ml^2 \omega_0^2}, \quad \omega = \frac{\omega_w}{\omega_0}$$

Bearing in mind such model assumptions, it is also necessary to take into account the factor that causes the movement. In the case under consideration, the pendulum was forced to move by means of a harmonic moment $M = p \cos(\omega\tau)$. Such a method of forcing the movement of the load can be accomplished by appropriate control of the hoisting mechanism winch. In the further part of the publication, the results of computer simulations, which allow the assessment of the impact of the mathematical models accepted for research on the motion of the transported load,

are illustrated in the form of time-course graphs, multi-colored maps of the maximum Lyapunov exponent, bifurcation diagrams, and Poincare cross-sections.

3. Results of model simulations

The results of computer simulations included in this chapter were obtained for two characteristic models representing the dynamics of the crane load movement. In order to illustrate the complex non-linear dynamics of the load movement, research tools enabling determination of chaotic motion zones were used. The effect of damping on the structure of the Poincare cross section and the largest Lyapunov exponent was also examined. The simulations were performed assuming a mass (crane lifting capacity) of 12.5t and length of the rope (hoisting height) 10m and zero initial conditions defining the speed $\dot{\varphi}(0)=0$. In the generalized coordinate, the initial angular displacement was assumed as $\varphi(0)=1^\circ$.

3.1. Results of the model without crane structure vibrations included

Influence of nonlinear model parameters on its dynamics is depicted in the form of multi-coloured map of largest Lyapunov exponent (Fig. 2). Based on them, it is possible to determine the zones in which the movement of the transported load is chaotic. Sample bifurcation diagrams are shown in Fig. 3.

The influence of the dimensionless external amplitude on the drawn image of the attractor is shown in the diagram (Fig. 4, a). Analogous tests were performed with respect to the dimensionless damping factor (Fig. 4, b). Having in view of obtaining an acceptable resolution, 160000 simulations were performed, which mapped the different conditions of input function affecting the load to the analyzed model. On the other hand, in relation to maps and graphs of the largest Lyapunov exponent, the graphic images were obtained assuming a constant distance $\varepsilon = 0,0001$, between the conditions characterizing the displacement and the initial velocity.

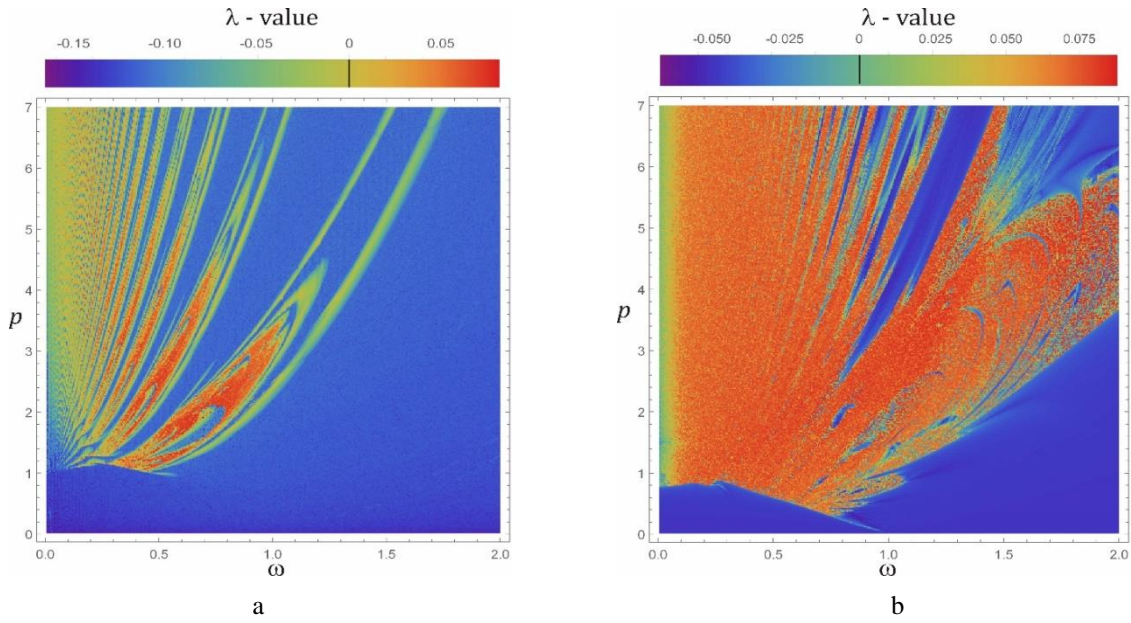


Fig. 2 Largest Lyapunov exponent maps: a) $\beta = 0.7$, b) $\beta = 0.1$

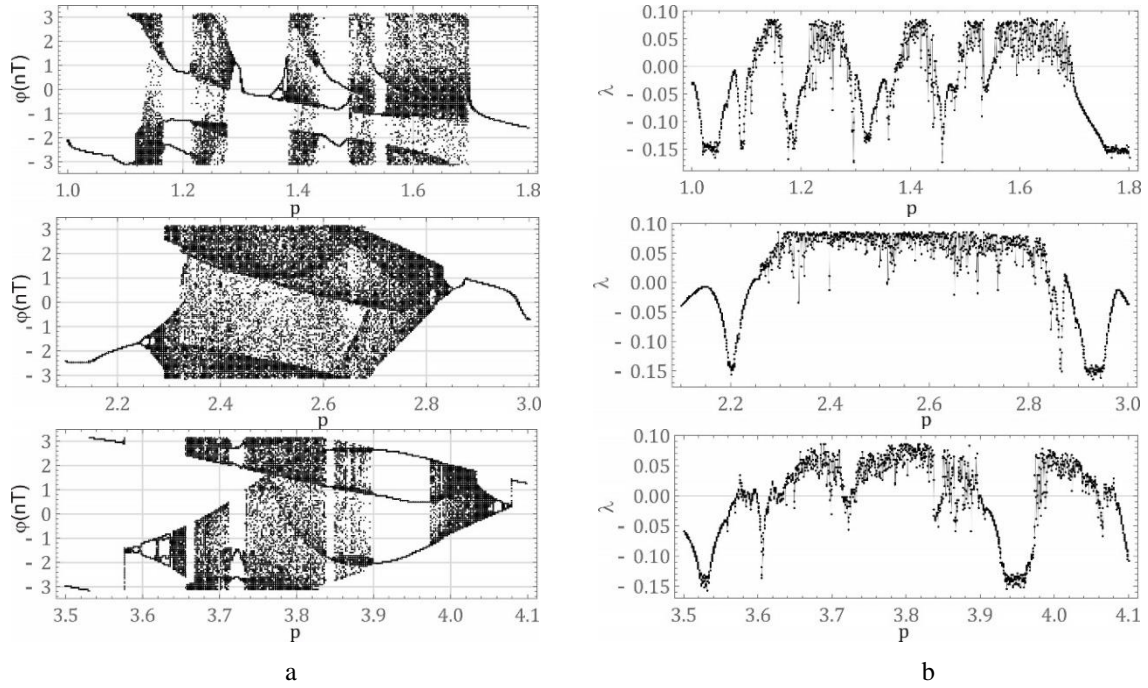


Fig. 3 Diagrams assuming the following parameters $\beta = 0.7$, $\omega = 0.5$, a) bifurcation diagrams, b) largest Lyapunov exponent

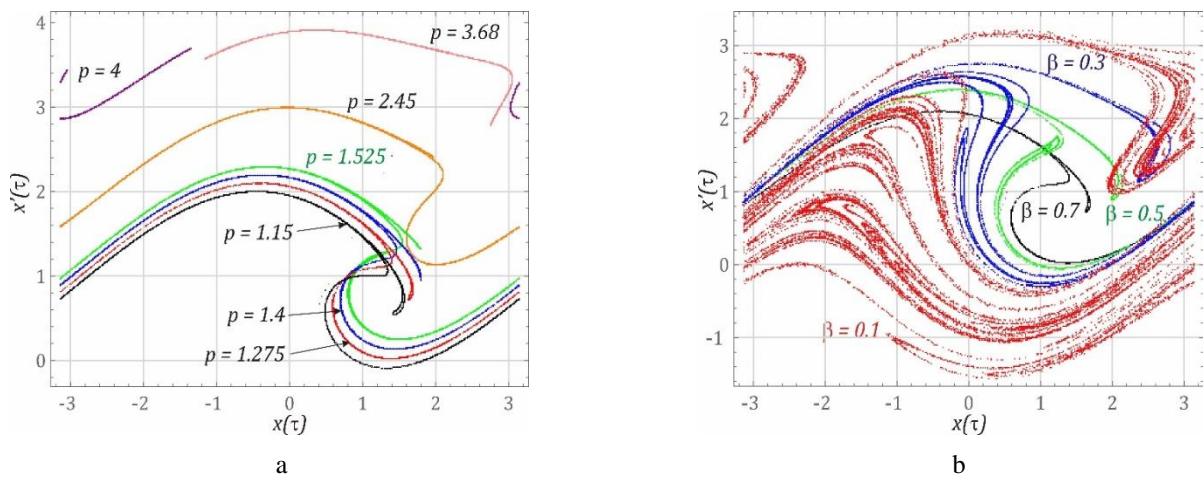
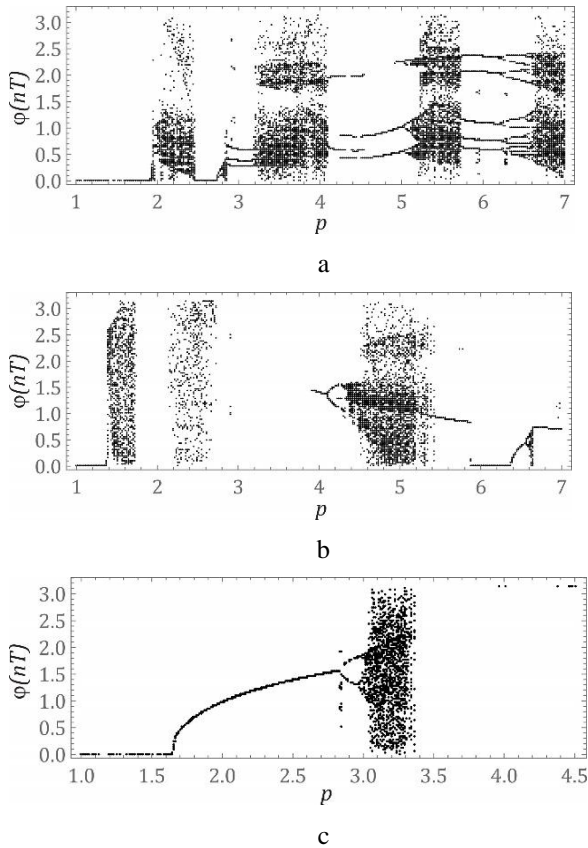


Fig. 4 Graphical representations of attractors based on the assumption of the following parameters: a) $\beta = 0.7$, $\omega = 0.5$, $p = 1.275$, $\omega = 0.5$

3.2. Results of the model with crane structure vibrations included

Based on the analytical relationships presented, computer simulations were conducted, the main purpose of which was to evaluate the influence of particular parameters of the mathematical model on the dynamics of the transported load. In the first stage of model research, areas where the system may behave chaotically are defined. For this purpose, a multi-coloured map of the distribution of largest Lyapunov exponents was generated (Fig. 5).



When the model is forced by harmonic kinematic force: $p = 1.63$, $\omega = 1.48$ and dimensionless damping factor value is $\beta = 0.628$, there are two stable orbits on the phase plane. Orbits were assigned to the corresponding basins of attraction (Fig. 6).

The blue areas represent the collection of initial conditions for the orbit in red. Even though both orbits have a geometrical similarity, their corresponding trajectories of motion in the x - y plane are different.

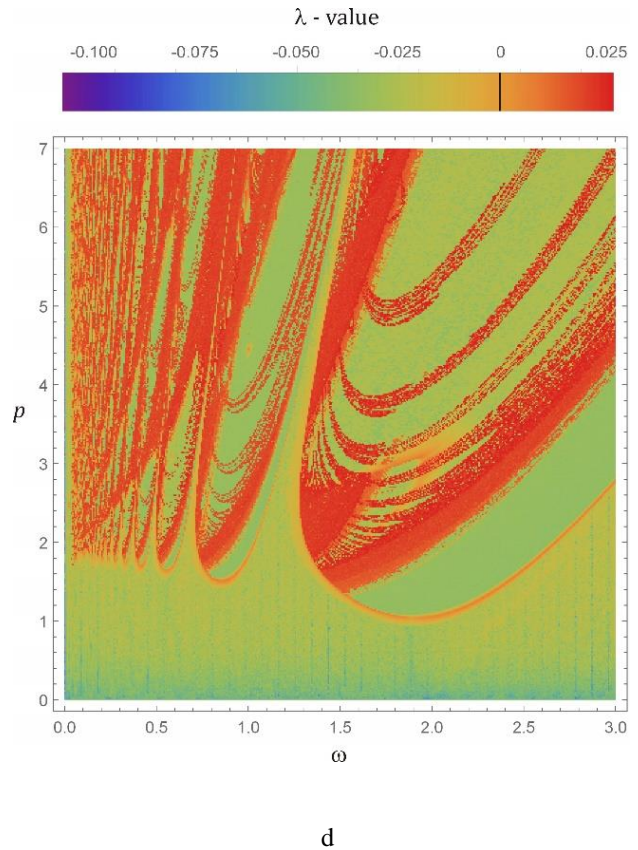


Fig. 5 Results of model tests: a) bifurcation diagram $\omega = 0.5$, b) bifurcation diagram $\omega = 1.5$, c) bifurcation diagram $\omega = 2.5$, d) Multi-coloured map of the largest Lyapunov exponent distribution $\beta = 0.5$

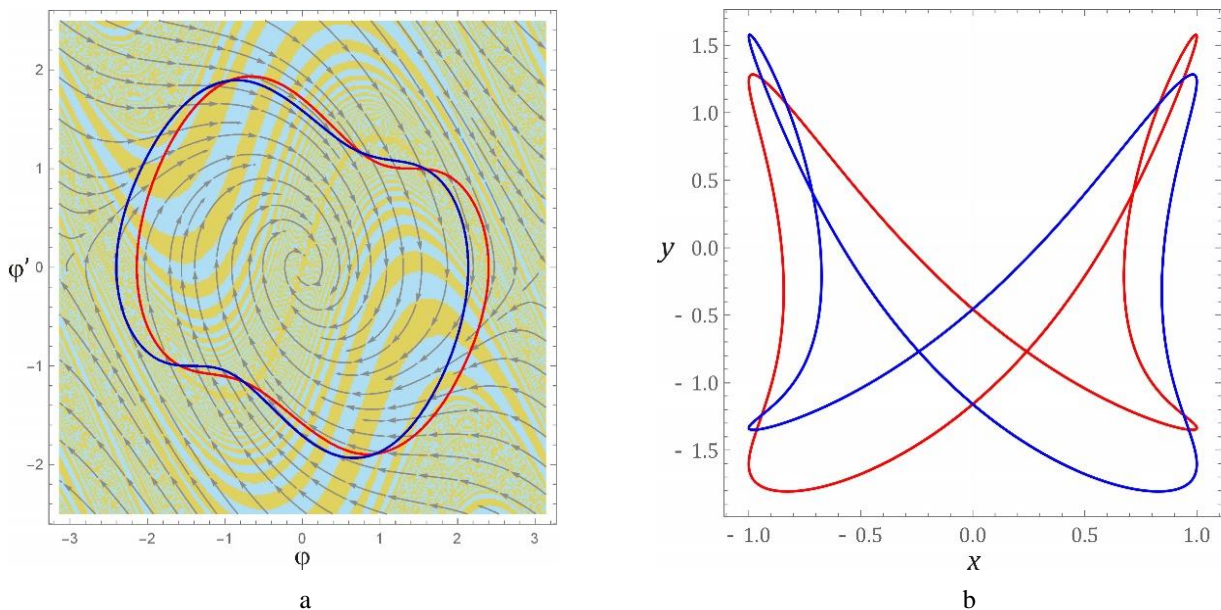


Fig. 6 Results of model tests $p = 1.63$, $\omega = 1.48$, $\beta = 0.628$: a) basins of attraction, b) trajectories of load movement in x - y plane

The results of numerical calculations illustrating the chaotic behaviour of the studied system are presented in the following part of the paper. The impact of the parameter p on the structure of the Poincare cross-section was investigated (Fig. 7, Fig. 8).

During the sensitivity testing of the system due to the initial conditions, a fixed distance $\varepsilon = 0.0001$ in moment $\tau[0]$ was assumed, between two trajectories. Attractor of the Poincare shape resembles the symbol of Chinese philosophy Yin and Yang (Figs. 7, a and 8, a).

4. Conclusions

On the basis of computer simulations, it is possible to formulate the following conclusions:

1. There is no chaotic phenomenon in the model taken into the study if the operator properly and in accordance with the manufacturer's guidelines operate the crane.

2. The increase in the damping coefficient representing the loss of energy in the structural node in which the rope connects to the drum has a significant effect on the "areas" of the dynamic excitation parameters values in which phenomena with chaotic nature may occur (Fig. 2).

3. Limiting the damping coefficient causes the Poincare cross-section, seen in the phase plane, to adopt a complex structure (Fig. 4, b).

4. The increase in the dimensionless amplitude of the kinematic excitation p results in higher harmonics in the frequency-amplitude spectrum (Figs. 7, c and 8, c), and Poincare cross-section shows a more complex structure.

5. The system is sensitive to initial conditions. The proximity of initial conditions can lead to different stable orbits, as shown in the graphs (Fig. 6, a). At the same time, the parameters of the mathematical model have a significant influence on the shape of the basins of attraction. On the other hand, plotted trajectories in the x - y plane of motion are mirrored (Fig. 6, b).

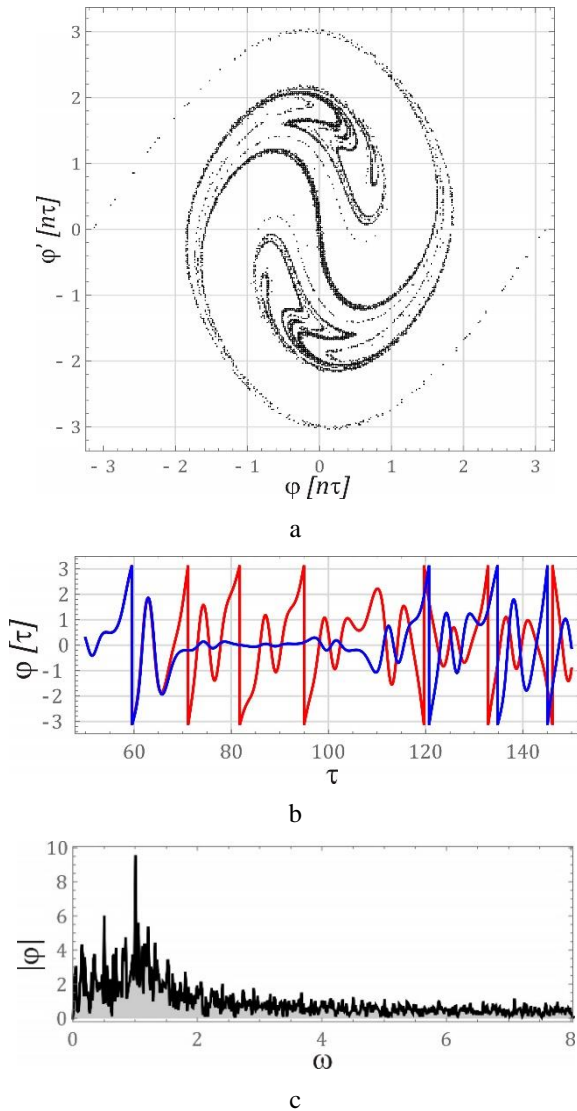


Fig. 7 Results of model tests $p = 1.68$, $\omega = 0.5$, $\beta = 0.1$: a) Poincare cross-section, b) timeline showing sensitivity to initial conditions, c) amplitude-frequency spectrum

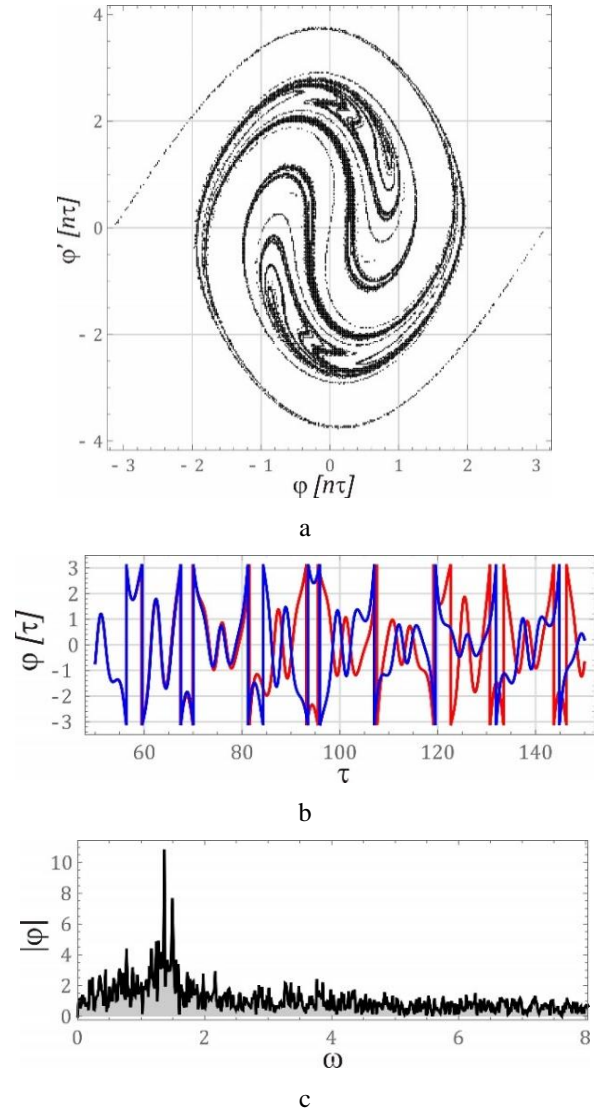


Fig. 8 Results of model tests $p = 3$, $\omega = 0.5$, $\beta = 0.1$: a) Poincare cross-section, b) timeline showing sensitivity to initial conditions, c) amplitude-frequency spectrum

References

1. **Ramli, L.; Mohamed, Z.; Abdullahi, A. M.; Jaafar, H. I.; Lazim I. M.** 2017. Control strategies for crane systems: A comprehensive review, *Mechanical Systems and Signal Processing* 95: 1-23. <http://dx.doi.org/10.1016/j.ymssp.2017.03.015>.

2. **Kosucki, A.; Malenta, P.; Stawiński, L.; Halusiak, S.** 2017. Energy consumption and overloads of crane hoisting mechanism with system of reducing operational loads, *Eksploatacja i Niezawodność – Maintenance and Reliability* 19(4): 508–515.
<http://dx.doi.org/10.17531/ein.2017.4.3>.
3. **Gaska, D.; Margielewicz, J.; Haniszewski, T.; Matyja, T.; Konieczny, L.; Chróst, P.** 2015. Numerical identification of the overhead travelling crane's dynamic factor caused by lifting the load off the ground, *International Journal of Measurements in Engineering* 3(1): 1–8.
4. **Smoczek, J.; Szpytko, J.; Hyla, P.** 2012. The Application of an Intelligent Crane Control System, 13th IFAC Symposium on Control in Transportation Systems: 280–285.
5. **Kim, D.; Singhose, W.** 2010. Performance studies of human operators driving double-pendulum bridge cranes, *Control Engineering Practice* 18: 567–576.
<http://dx.doi.org/10.1016/j.conengprac.2010.01.011>.
6. **Han, N.; Cao, Q.** 2017. Rotating pendulum with smooth and discontinuous dynamics, *International Journal of Mechanical Sciences* 127: 91–102.
<http://dx.doi.org/10.1016/j.ijmecsci.2016.09.024>.
7. **Náprstek, J.; Fischer, C.** 2013. Types and stability of quasi-periodic response of a spherical pendulum, *Computers and Structures* 124: 74–87.
<http://dx.doi.org/10.1016/j.compstruc.2012.11.003>.
8. **Hannan, M. A.; Bai, W.** 2016. Analysis of nonlinear dynamics of fully submerged payload hanging from offshore crane vessel, *Ocean Engineering* 128: 132–146.
<http://dx.doi.org/10.1016/j.oceaneng.2016.10.030>.
9. **Litak, G.; Syta, A.; Budhraj, M.; Saha, L. M.** 2009. Detection of the chaotic behaviour of a bouncing ball by the 0–1 test, *Chaos, Solitons and Fractals* 42: 1511–1517.
<http://dx.doi.org/10.1016/j.chaos.2009.03.048>.
10. **Krasilnikov, P.; Gurina, T.; Svetlova, V.** 2018. Bifurcation study of a chaotic model variable-length pendulum on a vibrating base, *International Journal of Non-Linear Mechanics*.
<https://doi.org/10.1016/j.ijnonlinmec.2018.06.011>.
11. **Figlus, T.** 2015. The application of a continuous wavelet transform for diagnosing damage to the timing chain tensioner in a motorcycle engine, *Journal of Vibroengineering* 17(3): 1286–1294.
12. **Margielewicz, J.; Gaska, D.; Wojnar, G.** 2017. Numerical modelling of toothed gear dynamics. *Scientific Journal of Silesian University of Technology. Series Transport* 97: 105–115.
<https://doi.org/10.20858/sjsutst.2017.97.10>.
13. **Arena, A.; Casalotti, A.; Lacarbonara, W.; Cartmell, M. P.** 2015. Dynamics of container cranes: three-dimensional modeling, full-scale experiments and identification, *International Journal of Mechanical Sciences* 93: 8–21.
<http://dx.doi.org/10.1016/j.ijmecsci.2014.11.024>.

J. Margielewicz, D. Gaska, T. Opasiak, T. Haniszewski

NUMERICAL STUDIES OF THE OVERHEAD TRAVELLING CRANES LOAD MOTION

S u m m a r y

The paper presents the results of numerical investigations of the overhead travelling cranes load motion. The model studies assume that the load is suspended on the inextensible rope. Conversely, its motion is triggered by an external moment. In addition, energy losses in the construction node connecting the rope to the drum are included. At the same time these losses were mapped through a linear viscous damper. The main objective was to evaluate the impact of individual mathematical model parameters on the dynamics of the transported load. The results were compared between two models: with/without crane structure vibrations included. The results were illustrated by multi-colored maps of the largest Lyapunov exponent, bifurcation diagrams, and Poincare cross-sections.

Keywords: chaos, mechanical vibration, cranes, modelling, Lyapunov exponent.

Received July 24, 2018

Accepted June 14, 2019